Annales
Geophysicae

Four-point high time resolution information on electron densities by the electric field experiments (EFW) on Cluster

A. Pedersen[1], P. Decreau[2], C.-P. Escoubet[3], G. Gustafsson[4], H. Laakso[3], P.-A. Lindqvist[5], B. Lybekk[1], A. Masson[3], F. Mozer[6], and A. Vaivads[4]

[1]University of Oslo, Norway
[2]LPCE/CNES, Orleans, France
[3]Space Science Department, ESTEC, Noordwijk, The Netherlands
[4]University of Uppsala, Sweden
[5]Royal Institute of Technology, Stockholm, Sweden
[6]SSL, University of California, Berkeley, USA

Abstract. For accurate measurements of electric fields, spherical double probes are electronically controlled to be at a positive potential of approximately 1 V relative to the ambient magnetospheric plasma. The spacecraft will acquire a potential which balances the photoelectrons escaping to the plasma and the electron flux collected from the plasma. The probe-to-plasma potential difference can be measured with a time resolution of a fraction of a second, and provides information on the electron density over a wide range of electron densities from the lobes ($\sim 0.01\,\mathrm{cm}^{-3}$) to the magnetosheath ($> 10\,\mathrm{cm}^{-3}$) and the plasmasphere ($> 100\,\mathrm{cm}^{-3}$). This technique has been perfected and calibrated against other density measurements on GEOS, ISEE-1, CRRES, GEOTAIL and POLAR. The Cluster spacecraft potential measurements opens the way for new approaches, particularly near boundaries and gradients where four-point measurements will provide information never obtained before. Another interesting point is that onboard data storage of this simple parameter can be done for complete orbits and thereby will provide background information for the shorter full data collection periods on Cluster. Preliminary calibrations against other density measurements on Cluster will be reported.

Key words. Magnetospheric physics (magnetopause, cusp, and boundary layers) Space plasma physics (spacecraft sheaths, wakes, charging; instruments and techniques)

1 Introduction

Most spacecraft have solar cells and thermal blankets made of highly resistive materials. Sunlit surfaces tend to charge to positive potentials due to the emission of photoelectrons, and shadowed surfaces charge to negative potentials due to the collection of ambient electrons. In the case of high fluxes of energetic electrons, this negative potential will dominate.

The ESA GEOS-1 and the NASA ISEE-1 and ISEE-2 spacecraft, all launched in 1977, were the first to have conductive surfaces in order to support electric field and low energy particle measurements. The conductivity required for this purpose is of the order of $0.1\,\mathrm{M\Omega}$ between sunlit and shadowed surfaces and their integrated connection to the structure and the electric reference point (star point). This is sufficient for most magnetospheric and solar wind environments to ensure that the spacecraft surfaces have a uniform potential within better than 1 V. This potential relative to the ambient plasma will be determined by a balance between the photoelectrons escaping to the plasma and the ambient electrons collected by the spacecraft. A high flux of electrons in the plasmasphere, the magnetosheath and in the solar wind will bring such a spacecraft to a few volts positive relative to the plasma. In the lobes, the electron flux is very low and the spacecraft will go very positive and cause most photoelectrons to orbit back to the spacecraft; only the high energy tail of the photoelectron distribution will balance the ambient electrons, and spacecraft potentials of $+50\,\mathrm{V}$ or more can then be observed. Ion currents are always negligible compared to photoelectron and electron currents, in the high speed solar wind as well.

Electric field spherical double probe experiments have been, or are at present in operation (GEOS-1, GEOS-2, ISEE-1, CRRES, GEOTAIL, POLAR and Cluster). For the proper operation of an electric field experiment, it is necessary to force electrons to the probes by a high impedance current source, thereby placing them close to the plasma potential. In this way, they have an optimum impedance for connecting to the plasma. This is necessary for electric field measurements, and in addition, it provides a potential reference for the spacecraft. For detailed explanations, see Pedersen et al. (1998). The potential between the spacecraft and an

Correspondence to: A. Pedersen
(arne.pedersen@fys.uio.no)
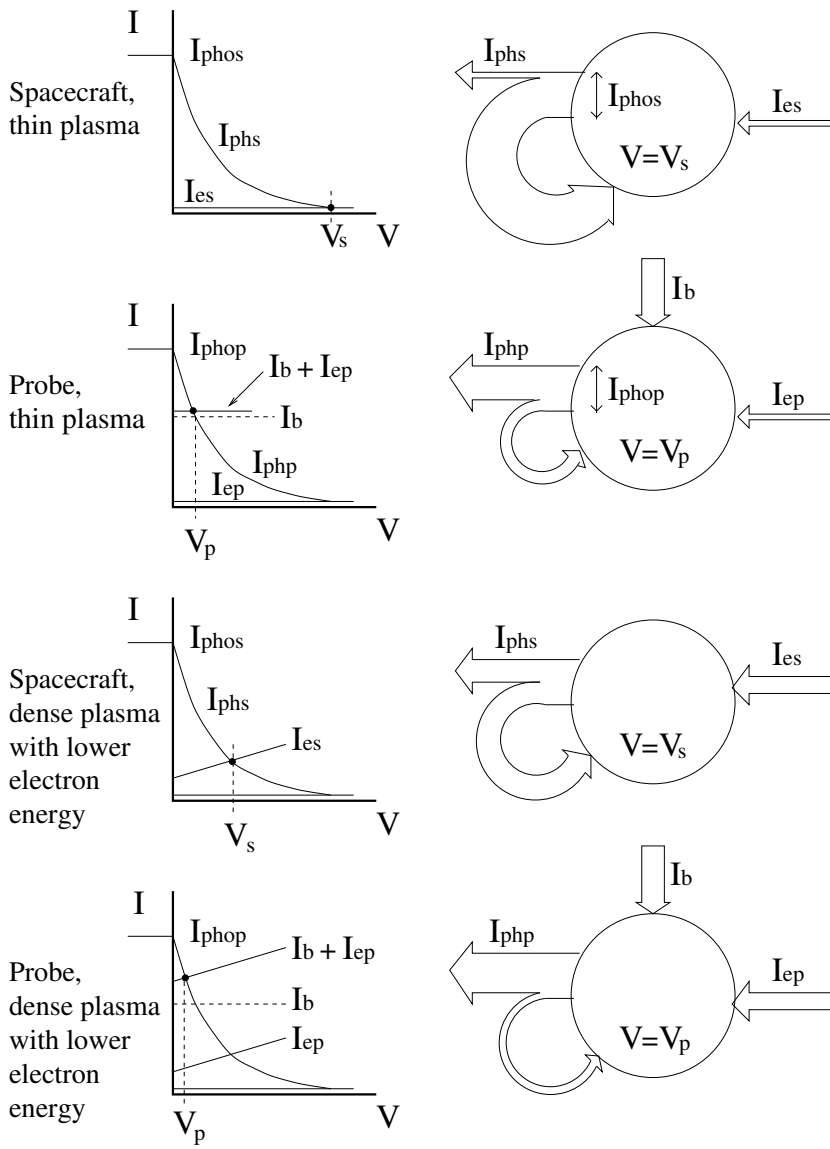
Fig. 1. Schematic illustrations of the spacecraft and probe current balance between photoelectrons escaping to the plasma and electrons collected from the plasma. For the probe, a bias current (I_b) forces electrons to the probe independent of probe voltage. I_{phos} and I_{phop} are spacecraft and probe photoelectron saturation currents. I_{phs} and I_{php} are spacecraft and probe photoelectron currents as functions of, respectively, spacecraft potential (V_s) and probe potential (V_p). I_{es} and I_{ep} are spacecraft and probe electron currents as functions of, respectively, V_s and V_p.

electric field probe has been related to the plasma density and the electron flux in different plasma environments (Laakso et al., 1995; Pedersen, 1995; Escoubet et al., 1997; Nakagawa et al., 2000; Scudder et al., 2000). More details about the electric field experiment (EFW) are given by Gustafsson et al. (1997) and by Andre et al. (2001, this issue).

This technique cannot compete with particle experiments or active or passive wave experiments for the accurate determination of plasma parameters. Its usefulness, following the calibration by these experiments, is the ability to measure rapid changes in plasma density or electron flux at boundaries with a time resolution better than 0.1 s. Furthermore, the spacecraft potential measurements can be used as an easy survey parameter, and can also be extrapolated to very low density environments (lobes) where particle experiments acquire very few counts.

2   Calibration of spacecraft potential measurements on Cluster

All electric field probes on Cluster are 8 cm in diameter spheres with a uniform carbon-paint surface. The best method to find the photoelectron characteristic for one sphere is to choose a tenuous plasma environment and step the bias current (electrons forced onto the sphere) until the sphere rushes to negative potentials; this happens when the bias current exceeds the maximum photoelectron current, where all photoelectrons from the probe will then escape to the plasma. Figure 1 is a schematic presentation of the current balance for the spacecraft and one of the electric field probes in respectively a thin plasma and a more dense plasma with lower electron energy. The maximum photoelectron currents emitted by the spacecraft and the probe are I_{phos} and I_{phop}. The current scale for the spacecraft is approximately 1000 times

that for the probe. For the spacecraft, the escaping photoelectrons (I_{phs}) are in balance with the collected ambient electrons (I_{es}), resulting in a potential V_s. For the probe, the negative bias current (I_b), which forces the electrons on the probe, plus the collected ambient electrons (I_{ep}), balance the escaping photoelectrons (I_{php}) from the probe. This causes the probe to be at a potential V_p close to that of the plasma, with only a small variation from a thin plasma to a more dense plasma.

In Fig. 2, it is shown that the maximum probe photoelectron current, I_{phop}, is 280 nA, corresponding to a current density $J_{pho} = 56\,\mu\mathrm{Am}^{-2}$, and that the e-folding energy of the photoelectrons, eV_{ph}, is 3 eV, as determined from probe bias current sweeps which forces the probe to be at a few volts positive relative to the plasma. This value of I_{phop} was the one at the end of 2000; previous studies have demonstrated that it will increase and gradually reach a stable value over approximately one year. Stable values of I_{pho} above 300 nA can be expected (Schmidt and Pedersen, 1987). In order to follow this development, it is necessary to repeat the calibration procedure at intervals.

The escaping part of the photoelectrons is $I_{php} = I_{phop}$ $\exp(V/V_{ph})$. In Fig. 2, typical bias currents of 172 nA and 220 nA are drawn. In a tenuous plasma, this will position the probe at the potentials of, respectively, $V_P = 1.2$ V and $V_P = 0.7$ V relative to the plasma. V_p is determined from balance between the photoelectron characteristic and the bias current chosen. When Cluster enters a more dense plasma, the ambient electron current will add to the bias current and drive the probe even closer to the plasma potential.

The spacecraft, including booms, have a sunlit area of approximately 5 m^2, which is 1000 times larger than the sunlit area of one probe. On GEOS-2, it was established that the photoemission current density from the spacecraft surfaces and the probes was very similar. This was done by observing that the potential difference between an unbiased probe and the spacecraft in a dense plasma was very small. In the absence of such a check on Cluster, we will assume that the maximum photoemission for the spacecraft is 280 μA, and that the e-folding energy of the photoelectrons for small positive potentials, in this case, is 3 eV.

The Whisper active plasma resonance experiment on Cluster (Decreau et al., 1997) provides information about the electron density. Simultaneous measurements of the electron density and the spacecraft-to-probe potential difference, $V_s - V_p$, is used in Fig. 2 to check the spacecraft photoelectron characteristic. We have chosen cases where the solar wind density, measured by Whisper, was 1, 10 and 20 cm^{-3}. The solar wind electron energy was chosen to be 16 eV; this choice is not critical for the following check. The more difficult choice is to establish the electron current collection area for Cluster (cylinder with a 3 m diameter and a 1.3 m height). The electron current to a sphere of radius r is $I_e = J_{eo}4\pi r^2$ $(1 + V/V_e)$, where J_{eo} is the random electron current and eV_e is the electron mean energy (Pedersen, 1995). Cluster is not a sphere; however, when the size of a body is smaller than the Debye length, the body attracts ambient electrons
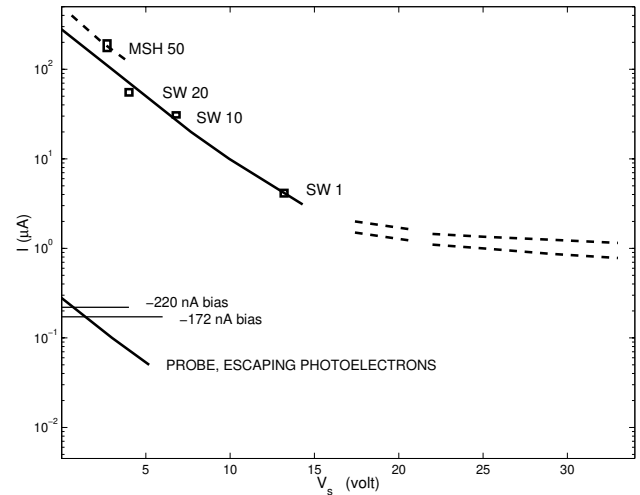
Fig. 2. Lower part: probe photoelectron current plotted against probe potential, and two bias curents of -172 nA and -220 nA. The current balance results in probe potentials of 1.2 V and 0.7 V, respectively. Upper part: spacecraft photoelectron characteristic, determined from Whisper solar wind and magnetosheath electron densities. Electron energy is assumed to be 16 eV in the solar wind and in the range of 30–50 eV in the magnetosheath. Symbols are the following: SW 1 is 1 cm^{-3}, SW 10 is 10 cm^{-3} and SW 20 is 20 cm^{-3} in the solar wind. MSH 50 is 50 cm^{-3} in the magnetosheath. The squares mark values of currents to the spacecraft for solar wind and magnetosheath plasma accelerated to the spacecraft for the corresponding measured $V_s - V_p$ values. The dotted lines are extensions of the photoelectron characteristics to spacecraft voltages up to 33 V. See text for detailed explanations.

like a sphere (Bourdeau et al., 1961). For this check, it is a satisfactory approximation since the spacecraft is smaller than the Debye length in all solar wind and magnetospheric environments except in the plasmasphere, when the electron density, N_e, exceeds approximately 50 cm^{-3}. The measured V_s values and the corresponding solar wind densities from Whisper ($N_e = 1$, 10 and 20 cm^{-3} marked SW 1, SW 10 and SW 20 in Fig. 2) have been used to calculate the current of the accelerated solar wind electrons to the spacecraft. The currents to the spacecraft, corresponding to the V_s values measured for the three solar wind electron densities, are given as squares in Fig. 2. The width of the squares indicates the uncertainty in the spacecraft potential relative to the plasma. In these calculation, we have assumed that the spacecraft electron collecting area is in the range of 20–25 m^2; this uncertainty is given as the height of the squares. The solar wind squares fit fairly well on a photoelectron characteristic with $I_{phos} = J_{phop} \cdot 5.0$ m^2 and an e-folding energy of 3 eV, demonstrating that the probe and the spacecraft have very similar characteristics at least up to V_s values of 10–15 V.

The electron drift instrument, EDI, on Cluster emits electrons with energy above 1 keV. For a period on 14 January 2001, EDI emitted 300 nA on spacecraft 2 when all spacecraft were in the magnetosphere (Paschmann, private communication). Other spacecraft with no electrons emitted from
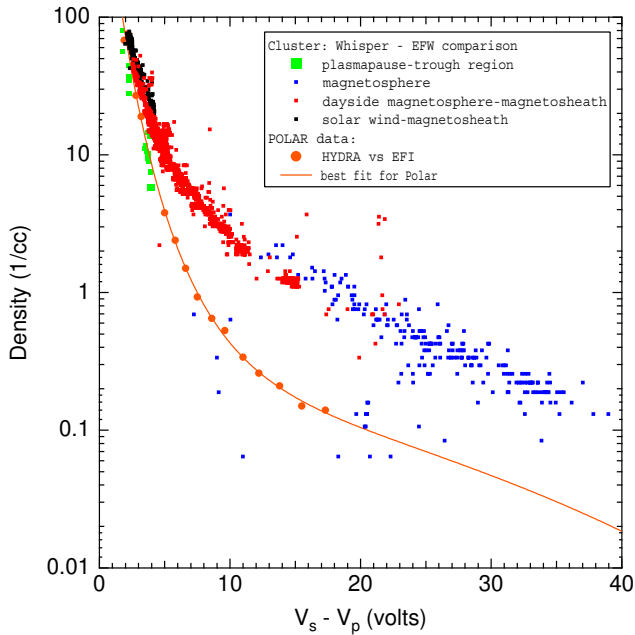
Fig. 3. Electron densities measured by Whisper given as a function of the spacecraft-to-probe potential difference, $V_s - V_p$. V_p is of the order of 1.0 volt in a tenuous magnetospheric plasma ($N_e < 1 \, \mathrm{cm}^{-3}$), and is less than 1.0 V relative to the plasma for higher electron densities.

EDI showed identical potentials relative to the plasma, but were less positive than on spacecraft 2. This observation can be used to see how much the spacecraft photoelectron current to the plasma must decrease to balance the EDI electron emission. By using periods with different plasma densities, and observing the differences between V_s for spacecraft 2 and the other spacecraft, it is possible to extend the spacecraft photoelectron characteristic to more positive potentials (dotted lines in Fig. 2). The upper and lower dotted lines indicate the uncertainty in this calculation. The spacecraft has higher e-folding energies for spacecraft potentials above 10–15 V. This is in agreement with previous observations (Escoubet et al., 1997). The normal operational EDI electron current is variable, but near 40 nA, and for spacecraft potentials with less than approximately +40 V, this is a negligible current. For very positive spacecraft potentials, corresponding to very tenuous plasmas, it may be necessary to consider if EDI is operating or not in order to obtain the best calibration between the spacecraft potential and the density or the electron flux.

During high densities in the magnetosheath, it was expected that the spacecraft would go to very small potentials, less than 1 V, and that the probes would be negative. This did not happen and the likely explanation is that the magnetosheath electrons, with energies up to 50 eV or possibly more, will produce secondary electrons with typical energies of a few volts. A secondary electron yield of 50% is possible. In Fig. 2, V_s is plotted for a measured density by Whisper of $50 \, \mathrm{cm}^{-3}$ in the magnetosheath, assuming an electron energy

of 50 eV. This value of V_s deviates from the curve established in the solar wind where the lower electron energy has a very small secondary electron yield. This deviation indicates a possible component of the secondary electrons in addition to photoelectrons in the magnetosheath. Secondary electrons are emitted with energies below 10 eV and are not important for very positive spacecraft potentials. The secondary electrons will, in this case, not escape, but will orbit back to the spacecraft.

In Fig. 3, the electron density from Whisper is given as a function of $V_s - V_p$. Data for each point in the plot have been taken from intervals when the plasma density was constant over a much longer time than the sampling intervals for EFW (1/5 s) and Whisper (1.5 s up to 28 s depending on the mode). The data has been selected from four days in the period from December 2000 to February 2001. Since V_p is close to the plasma potential, it makes sense to speak about electron density versus spacecraft potential. Numerical simulations by Escoubet et al. (1997) and Laakso and Pedersen (1998) have demonstrated that for low electron energies (plasmasphere and solar wind), $V_s - V_p$ is a function of density and a weak function of electron energy. Calibrated electron densities and energies have so far not been available on Cluster for tenuous plasmas where electron energies are higher and $V_s - V_p$ depends on electron density as well as energy. The POLAR electron density versus $V_s - V_p$ curve (Scudder et al., 2000), which is also shown in Fig. 3, is quite different from the Cluster curve which has higher current densities and higher e-folding energies for the escaping photoelectrons than for previous missions. The difference is more marked for lower electron densities and more positive spacecraft potentials. A possible explanation can be that the photoemission is more pronounced at solar maximum, when Cluster data was collected, than for the POLAR data collected closer to solar minimum. The POLAR curve in Fig. 3 is based on calibration with an electron experiment. It will be necessary in the future to check if Whisper overestimates, to some extent, the electron density in a tenuous plasma due to a possible influence from the photoelectrons around the spacecraft. The spread of blue data points (magnetosphere) in Fig. 3 is due to variations in electron energy. This dependance will be studied in the future with Cluster electron data.

3 Spacecraft potential measurements at the magnetopause

Before presenting examples of observations at the magnetopause, it is necessary to estimate the time, Δt, required for a spacecraft to come to an equilibrium when the plasma conditions change. We approximate the spacecraft capacitance C with a sphere of diameter $r = 1$ m, resulting in $C = 4\pi\epsilon r = 10^{-10}$ F. First, we consider a sudden change in the plasma density to a very small value. The current balance in this new situation will require that less photoelectrons escape to space, and they will instead orbit back to the spacecraft. This can only be achieved by a more positve spacecraft.
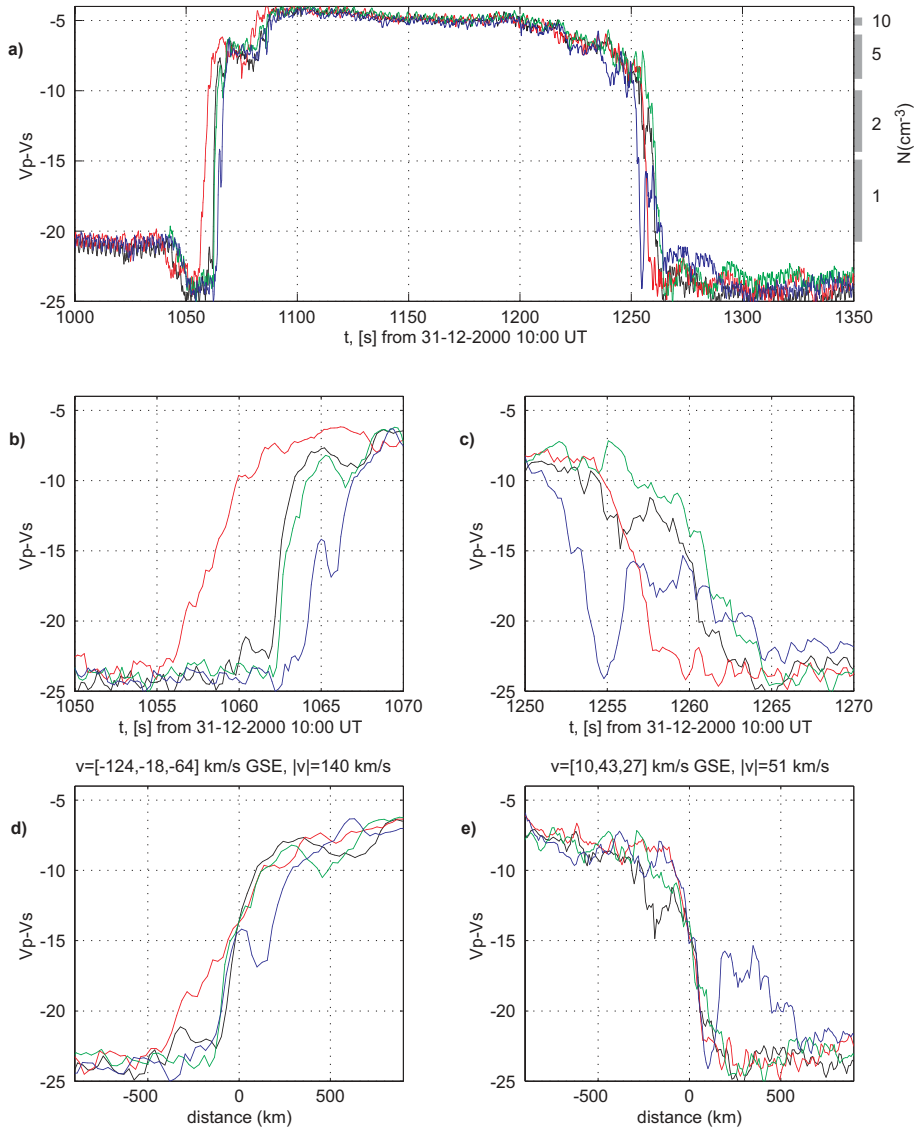
Fig. 4. Time series of the probe to spacecraft potential, $V_s - V_p$, for the four Cluster spacecraft (black is spacecraft 1, red is spacecraft 2, green is spacecraft 3 and blue is spacecraft 4) are given in panel (**a**). Panels (**b**) and (**c**) are the same as (a) for selected shorter intervals. Panels (**d**) and (**e**) show $V_s - V_p$ as a function of a distance scale parallel to an estimated magnetopause normal. The zero on this scale has been placed arbitrarily at the midpoint of the magnetopause boundary layer gradient. The magnetopause velocity vectors, in GSE coordinates, are also given in these two panels.

Typical orbital times of the bulk of the photoelectrons at low energies will be of the order of μs and the adjustment of currents is very fast. The charging time will be of the order of $\Delta t = C \cdot \Delta V / \Delta I_{ph}$, where ΔV is the voltage change and ΔI_{ph} is the reduction in photoelectrons emitted to space. For $\Delta V = 50$ volt and $\Delta I_{ph} = 10 \, \mu$A, $\Delta t = 0.5$ ms. This rough estimate only serves to demonstrate that t is very small. For a situation where the spacecraft moves from a very tenuous plasma to a denser one, $\Delta t = C \cdot \Delta V / \Delta I_{es}$, where I_{es} is the step in the ambient electron current. The increase of ambient electrons will in this case be balanced very quickly by emission of additional photoelectrons to the plasma from the large supply of photoelectrons on trapped orbits near the spacecraft. The most critical situation is in a tenuous plasma where the electron current is small and will be the limiting factor for balancing the photoelectron current increase. The following values give an indication: $\Delta V = 10$ V and ΔI_{es} 100 nA. This will result in $\Delta t = 10^{-2}$ s. It is interesting to note that in this

latter case, moving to a denser plasma, Δt is smaller for a large body than a small body because C is proportional to r, but the electron current is proportional to r^2.

It can safely be concluded that Δt is smaller than 0.1 s from the above rough estimates. A numerical simulation of how the spacecraft follows plasma gradients must be the next step for obtaining a better quantitative understanding of this problem. For more details, see Laakso et al. (1995).

All Cluster spacecraft experienced several magnetopause crossings on 31 December 2000 for more than four hours when Cluster orbited from 15.4 R_E to 17.5 R_E, and the magnetic latitude changed from 30.5° to 21.3°. The magnetic local time was close to 16:20 MLT for the whole period. One example from early in this period of an inward and then an outward motion of the magnetopause, observed as the spacecraft potential changed, is presented in Fig. 4. The parameter $V_p - V_s$, which is approximately $-V_s$, is plotted as a function of time; this makes it possible to associate an in-

crease in electron density with an upwards trend in $V_p - V_s$. An approximate density scale from Fig. 3 is given on the right side of Fig. 4a. The panels (b) and (c) in Fig. 4 show 20 s intervals covering, respectively, the inward and the outward motion of the magnetopause. André et al. (2001, this issue) have analysed the same event as the one shown in Fig. 4, with emphasis on low frequency waves and magnetic field data which demonstrates clear crossings of the magnetopause current layer. Spacecraft 4 observed that the magnetic field turned from northward to southward in the time interval 1240–1250 s after 10:00 UT, and from southward to northward in the time interval 1240-1250 s after 10:00 UT. Referring to the upper panel of Fig. 4, this indicates that the steep gradient is of the order of 5 s inside the inner edge of the current layer. We will later translate this into an approximate distance scale.

It is beyond the scope of this paper to present a detailed study of the magnetopause; this can only be done when data from more experiments can be combined. However, we can outline the possibilities and limitations of the spacecraft potential technique when crossing the boundary layer and the magnetopause current layer. The $V_p - V_s$ parameter, which, in normal mode, is sampled every 1/5 s, can resolve the fast density changes over one second, as seen for some bondary layer crossings in Fig. 4b. It is also possible to see boundary layer structure and to see that spacecraft 2 (red), which was at the greatest distance from the Earth, had a longer boundary layer crossing, indicating that the boundary moved more slowly for the spacecraft 2 crossing than for the following ones.

There is a drop in $V_p - V_s$ on all spacecraft from -22 V to -24 V for approximately 15–20 s before the first steep gradient in Fig. 4a. It is unlikely that there is a density depletion at the inner edge of the boundary layer; it is more likely that there is a drop in electron temperature when shifting from magnetospheric conditions to a region of colder magnetosheath plasma. This drop in $V_p - V_s$ is not seen for the outward motion of the magnetopause. In the steep density gradient, it is difficult to assess the electron energy distribution, and electron experiments may have problems with measurements in a short time period. This means that the exact densities through the gradient will be difficult to determine. However, all spacecraft will experience the same relation between electron density and $V_p - V_s$. In addition, the gradient measurements can be used for the relative timing of gradient crossings in order to estimate the normal to the magnetopause and the velocity of the magnetopause along this direction, using the assumption that the magnetopause is a plane on a scale comparable to the spacecraft separations, of the order of 500 km. Furthermore, it is necessary to assume that the magnetopause moves with a constant velocity across all spacecraft. Figures 4b and 4c show that this is not always the case. During the inward motion of the magnetopause, spacecraft 2 observes less steep changes in $V_p - V_s$ than the other spacecraft. At the same time, spacecraft 4 observes small-scale variations in the middle of the gradient that are not observed by the other spacecraft. The variations between

spacecraft are even larger during the outward motion of the magnetopause. Nevertheless, we can obtain a rough estimate of the magnetopause velocity using the above mentioned assumptions. For this we need to estimate the time separation between the boundary layer gradients for all spacecraft. Figures 4d and 4e give the velocity for the magnetopause inward motion to be 148 km/s (-128, -25, -72 km/s in GSE coordinates), and 51 km/s (10, 43, 27 km/s in GSE coordinates) for the outward motion. The same figures give the boundary layer gradient on a distance scale, where zero is placed in the middle of the gradient. For these plots, the estimated velocities and time separations have been used to place the observed gradients in the moving magnetopause frame of reference. The gradient observations have been time shifted by eye to give the best possible similarity between observations. These best timeshifts can then be used in an iterative process to obtain the best velocity vectors.

The velocity of 148 km/s for the inward magnetopause motion, combined with a 5 s delay from the foot of the boundary layer gradient to the inner edge of the current layer, indicates that the thickness of the boundary layer is approximately 750 km. The time interval for crossing the current layer, quoted above, corresponds to a current layer thickness of approximately 1500 km. For the magnetopause outward motion, the smaller velocity of 51 km/s, combined with a similar time between the inner edge of the current layer and the foot of the boundary layer gradient, indicates a thinner boundary layer. However, this indication is uncertain since the magnetopause and density gradient normals are more difficult to determine in this case.

In the magnetopause current layer, the electrons will drift, and if the drift velocity is large compared to the thermal velocity, the electron density versus the spacecraft potential relation may differ from the one presented in Fig. 3. A model magnetopause current layer, 500 km thick, with tangential opposite magnetic fields of 20 nT on each side, will have a current density of approximately $J_d = 10^{-6}$ Am^{-2}. For an electron density of $N_e = 10^7$ m^{-3}, the electron drift velocity (approximated by $v_d = J_d / N_e \cdot e$) will be 1.2 10^6 m/s. The magnetosheath electron population, which probably dominates at the magnetopause, has typical electron thermal velocities of 4–6 10^6 m/s, and only for an extreme magnetopause, with low electron density and a very large current, will this technique be influenced.

4   Conclusions

Preliminary calibrations of spacecraft potential measurements as a function of electron density and energy have been done using electron density data from Whisper, the plasma resonance sounder on Cluster. Whisper data were obtained in the solar wind and in the magnetosheath where the electron energy is sufficiently well-known for this calibration. In a more tenuous magnetospheric plasma, the spacecraft potentials, measured versus the Whisper electron densities, are more scattered because the spacecraft current balance is more

sensitive to the energy of the ambient electrons which varies considerably in the magnetosphere.

The photoemission of the electric field probes on Cluster can be checked by using a bias current to move the probes to the plasma potential near each probe. All photoelectrons will then escape to the plasma and the maximum photoelectron current can be measured; at the end of the year 2000, the probe photoelectron current density was $56\,\mu Am^{-2}$ and the e-folding energy was $3\,eV$ for probe potentials of a few volts relative to the plasma. The spacecraft photoelectron emitting area is about $5\,m^2$, which is 1000 times that of one probe $(50\,cm^2)$. The electron collecting area of the spacecraft is more uncertain due to its flat cylinder shape. Values of 20–25 m^2 are assumed. When using these values, together with Whisper solar wind data, the calculated voltages for the current balance between photoelectrons and ambient electrons agree with the above parameters for the spacecraft photoelectron characteristic. In the magnetosheath, it appears that secondary emission electrons, emitted with typical energies of a few volts, add to the photoemission.

Once the understanding of the spacecraft and probes is established, it helps to obtain a confidence in the relation between the electron density and the spacecraft potential shown in Fig. 3. The complete calibration of this technique towards lower densities in the plasmas sheet and in the lobes will have to wait until calibrated partcle data are available in these regions. The Cluster electron density as a function of $V_s - V_p$, the spacecraft to probe potential difference ($V_s - V_p \sim V_s$ because V_p is small), differs from previous missions. A possible explanation is that Cluster data samples were taken during solar maximum with a higher photoelectron yield.

The time resolution of the spacecaft potential measurements at gradients is better than 0.1 s. The spacecraft capacitance is of the order of $100\,pF$ and the currents involved are sufficiently large to achieve this. Such measurements on four spacecraft can provide information about density gradients and their motion at the magnetopause and at the bow shock, and thereby complement particle measurements which necessarily have lower time resolution. Combined with measurements of electrons, ions, and electric and magnetic fields, this will greatly advance magnetospheric boundary studies. An additional advantage is that this simple voltage measurement, which is easily accessible, can be used as a survey parameter.

References

André, M., Behlke, R., Wahlund, J.-E., Vaivads, A., Eriksson, A.-I., Tjulin, A., Carozzi, T. D., Cully, C., Gustafsson, G., Sundkvist, D., Khotyaintsev, Y., Cornilleau-Wehrlin, N., Rezeau, L., Maksimovic, M., Lucek, E., Balogh, A., Dunlop, M., Lindqvist, P.-A., Mozer, F., Pedersen, A., and Fazakerley, A.: Multi-spacecraft observations of broadband waves near near the lower hybrid frequency at the Earthward edge of the magnetopause, Ann. Geophysicae (this issue) 2001.

Bourdeau, R. E., Donley, J. L., Serbu, G. P., and Whipple, Jr., E. C.: Measurements of sheath currents and equilibrium potential on the Explorer VII satellite, J. Astronaut. Sci., 8, 65–73, 1961.

Decreau, P. M. E., Fergeau, P., Krasnosels'kikh, V., Leveque, M., Martin, Ph., Randriamboarison, O., Sene, F. X., Trotignon, J. G., Canu, P., and Mogensen, P. B.: Whisper, a resonance sounder and wave analyser: Performance and perspectives for the Cluster mission, Space Science Rev., 79, 157–193, 1997.

Escoubet, C. P., Pedersen, A., Schmidt, R., and Lindqvist, P.-A.: Density in the magnetosphere inferred from the ISEE-1 spacecraft potential, J. Geophys. Res., 102, 17 595–17 609, 1997.

Gustafsson, G., Bostrom, R., Holmgren, G., Lundgren, A., Stasiewicz, K., Ahlen, L., Mozer, F. S., Pankow, D., Harvey, P., Berg, P., Ulrich, R., Pedersen, A., Schmidt, R., Butler, A., Fransen, A., Klinge, D., Falthammar, C.-G., Linqvist, P.-A., Christenson, S., Holtet, J., Lybekk, B., Sten, T. A., Tanskanen, P., Lappalainen, K., and Wygant, J.: The electric field experiment for the Cluster mission, Space Sci.Rev., 79, 137–156, 1997.

Laakso, H. and Pedersen, A.: Ambient electron density derived from differential potential measurements, in Measurement Techniques in Space Plasmas, AGU Geopys. Monograph, 102, 49–54, 1998.

Laakso, H., Aggson, T., and Pfaff, Jr., R. F.: Plasma gradient effects on double probe measurements in the magnetosphere, Ann. Geophysicae, 13, 130–146, 1995.

Nakagawa, T., Ishii, T., Tsuruda, K., Hayakawa, H., and Mukai, T.: Net current density of photoelectrons emitted from the surface of the GEOTAIL spacecraft, Earth Planets Space, 52, 283–292, 2000.

Pedersen, A.: Solar wind and magnetosphere plasma diagnostics by spacecraft electrostatic potential measurements, Ann. Geophysicae, 13, 118–121, 1995.

Pedersen, A., Mozer, F., and Gustafsson, G.: Electric field measurements in a tenuous plasma with spherical double probes, in Measurement Techniques in Space Plasmas, AGU Geophys. Monograph 103, 1–12, 1998.

Scudder, J. D., Cao, X., and Mozer, F.: Photoemission current-spacecraft voltage relation: Key to routine quantitative low energy plasma measurements, J. Geophys. Res., 105, 21 281–21 294, 2000.

Schmidt, R. and Pedersen, A.: Long-term behaviour of photoelectron emission from the electric field double probe sensors on GEOS-2, Planet Space Sci., 35, 61–70, 1987.